Electronic Supplementary Material (ESI) for Physical Chemistry Chemical Physics.

Electronic supplementary information for…

1-Alkyl-3-Methylimidazolium Cation Binding Preferences in Hexafluorophosphate Ionic Liquid Clusters Determined Using Competitive TCID Measurements and Theoretical Calculations

H. A. Roy and M. T. Rodgers*
Department of Chemistry, Wayne State University, Detroit, MI, 48202, USA

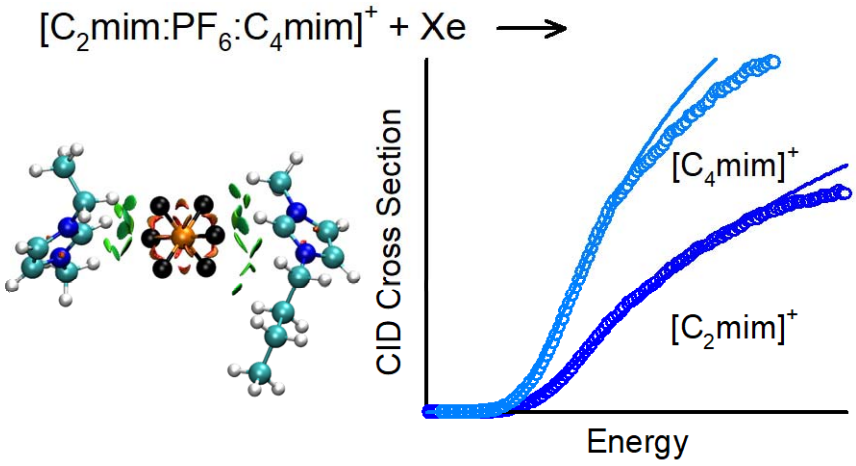

Table of Contents

Table S1. CID Fragments of the $[C_{n-2}mim:PF_6:C_nmim]^+$ Cluster Ions.[a]

precursor ion	m/z (Da/*e*)	symbol	1° fragment ion	2° fragment ions	neutral loss(es)
$[C_2mim:PF_6:C_4mim]^+$	395				
	139	●	$[C_4mim]^+$		$(C_2mim:PF_6)$
	111	●	$[C_2mim]^+$		$(C_4mim:PF_6)$
	83	□		$[C_4H_7N_2]^+$	C_4H_8
	57	△		$[C_4H_9]^+$	$C_4H_6N_2$
$[C_4mim:PF_6:C_6mim]^+$	451				
	167	●	$[C_6mim]^+$		$(C_4mim:PF_6)$
	139	●	$[C_4mim]^+$		$(C_6mim:PF_6)$
	83	□		$[C_4H_7N_2]^+$	C_6H_{12}
	57	△		$[C_4H_9]^+$	$C_6H_{10}N_2$
	43	○		$[C_3H_7]^+$	$C_7H_{12}N_2$
$[C_6mim:PF_6:C_8mim]^+$	507				
	195	●	$[C_8mim]^+$		$(C_6mim:PF_6)$
	167	●	$[C_6mim]^+$		$(C_8mim:PF_6)$
	83	□		$[C_4H_7N_2]^+$	C_8H_{16}
	71	▽		$[C_5H_{11}]^+$	$C_7H_{12}N_2$
	57	△		$[C_4H_9]^+$	$C_8H_{14}N_2$
	43	○		$[C_3H_7]^+$	$C_9H_{12}N_2$

[a]The elemental compositions of the $[C_nmim]^+$ cations are $[C_2mim]^+ = [C_6H_{11}N_2]^+$, $[C_4mim]^+ = [C_8H_{15}N_2]^+$, $[C_6mim]^+ = [C_{10}H_{19}N_2]^+$, and $[C_8mim]^+ = [C_{12}H_{23}N_2]^+$.

Table S2. Geometric Parameters of the B3LYP, B3LYP-GD3BJ, and M06-2X Ground Conformers of the $[C_n mim]^+$ Cations[a]

cation	theory	a1	a2	a3	a4	a5	a6	a7
$[C_2mim]^+$	B3LYP	-104.6						
	B3LYP-GD3BJ	-104.6						
	M06-2X	-108.0						
$[C_4mim]^+$	B3LYP	-100.1	-179.7	-179.6				
	B3LYP-GD3BJ	-103.5	61.9	177.3				
	M06-2X	-106.2	59.1	175.5				
$[C_6mim]^+$	B3LYP	-102.1	180.0	180.0	180.0	180.0		
	B3LYP-GD3BJ	-104.5	60.9	176.4	179.5	179.7		
	M06-2X	-106.4	58.9	174.0	179.2	179.4		
$[C_8mim]^+$	B3LYP	-103.0	179.3	179.8	179.5	180.0	179.7	180.0
	B3LYP-GD3BJ	-103.4	60.5	176.1	179.5	179.6	180.0	179.9
	M06-2X	-104.9	59.2	174.7	180.0	179.8	179.6	180.0

[a]The torsion angles are given in (°) and describe the 1-alkyl dihedral angles: a1 = ∠C2N1C1′C2′, a2 = ∠N1C1′C2′C3′, a3 = ∠C1′C2′C3′C4′, a4 = ∠C2′C3′C4′C5′, a5 = C3′C4′C5′C6′, a6 = C4′C5′C6′C7′, and a7 = ∠C5′C6′C7′C8′ as shown in **Figure S1**. The optimized structures were determined using the density functional indicated with a 6-311+G(d,p) basis set and are shown in **Figure 4**.

Table S3. Geometric Parameters of B3LYP, B3LYP-GD3BJ, and M06-2X Optimized Geometries of the $[BF_4]^-$ and $[PF_6]^-$ Anions[a]

theory	$[PF_6]^-$				$[BF_4]^-$		
	P-F (Å)	∠FPF (°)	cis F-F (Å)	trans F-F (Å)	B-F (Å)	∠FBF (°)	F-F (Å)
B3LYP	1.646	90.0	2.327	3.291	1.417	109.5	2.314
B3LYP-GD3BJ	1.645	90.0	2.327	3.291	1.417	109.5	2.314
M06-2X	1.628	90.0	2.303	3.257	1.410	109.5	2.302

[a]The optimized structures were determined using the density functional indicated with a 6-311+G(d,p) basis set and are shown in **Figure 4**. Ideal tetrahedral geometry observed for $[BF_4]^-$ and ideal octahedral geometry observed for $[PF_6]^-$ resulting in identical bond lengths and bond angles in the respective anion.

Table S4. Geometric Parameters of the B3LYP, B3LYP-GD3BJ, and M06-2X Ground Conformers of the ($C_n$mim:PF_6) Ion Pairs[a]

ion pair	theory	∠C2N3C1″H	a1[b]	∠C2HP	b[c]	b1[d]
(C_2mim:PF_6)	B3LYP	-4.8	-93.9	119.7	-3.9	46.6
	B3LYP-GD3BJ	28.4	113.0	102.5	-1.2	58.6
	M06-2X	-22.8	-116.8	92.6	-1.3	-65.6
(C_4mim:PF_6)	B3LYP	-16.7	-94.1	120.8	0.5	49.4
	B3LYP-GD3BJ	14.7	-103.3	110.9	-0.2	-56.2
	M06-2X	-24.6	-112.9	93.8	-1.3	-64.0
(C_6mim:PF_6)	B3LYP	16.2	-103.5	121.3	0.1	-49.7
	B3LYP-GD3BJ	1.8	-122.8	116.0	-5.9	-47.3
	M06-2X	-25.1	-111.8	94.0	-1.1	-63.9
(C_8mim:PF_6)	B3LYP	15.4	-103.9	120.4	-0.0	-50.1
	B3LYP-GD3BJ	16.1	-78.3	114.4	-7.7	-52.2
	M06-2X	-24.9	-111.4	93.9	-1.2	-63.9
ion pair	theory	C1′H-F	C2H-F	C1″H-F	C2-F	C2-P
(C_2mim:PF_6)	B3LYP	2.264	2.273, 2.103	2.321	2.766	3.568
	B3LYP-GD3BJ	2.445	2.272, 2.311	2.673	2.691	3.462
	M06-2X	2.389	2.319, 2.372	2.590	2.683	3.382
(C_4mim:PF_6)	B3LYP	2.275	2.169, 2.202	2.255	2.758	3.575
	B3LYP-GD3BJ	2.418	2.221, 2.252	2.265	2.672	3.500
	M06-2X	2.354	2.322, 2.362	2.613	2.678	3.393
(C_6mim:PF_6)	B3LYP	2.498	2.154, 2.222	2.273	2.798	3.591
	B3LYP-GD3BJ	2.447	2.190, 2.208	2.230	2.702	3.524
	M06-2X	2.349	2.313, 2.378	2.633	2.677	3.397
(C_8mim:PF_6)	B3LYP	2.493	2.175, 2.216	2.281	2.779	3.584
	B3LYP-GD3BJ	3.405	2.075, 2.603	2.114	2.667	3.594
	M06-2X	2.356	2.311, 2.384	2.627	2.678	3.398

[a] Bond and dihedral angles are given in degrees (°), bond distances are given in Angstroms (Å). Optimized structures were determined using the density functional indicated with a 6-311+G(d,p) basis set. See **Figure S1** for additional details regarding the definitions of the dihedral angles. [b]First 1-alkyl dihedral angle a1 ≡ ∠C2N1C1′C2′. [c]Binding site dihedral angle defined as **b** ≡ ∠(C2,©,©+CP,P) where © denotes the centroid of the imidazolium ring. [d]Binding orientation dihedral angle defined as **b1** ≡ ∠C1″N3C2P.

Table S5. Geometric Parameters of the B3LYP, B3LYP-GD3BJ, and M06-2X Ground Conformers of the $[C_{n-2}mim:PF_6:C_nmim]^+$ Clusters[a]

system	theory	∠C2N3C1″H	a1[b]	∠C2HP	**b**[c]	**b1**[d]	**b2**[e]
$[C_2mim:PF_6:C_4mim]^+$	B3LYP	9.8	102.8	139.4	-0.6	-35.4	81.4
		-14.6	100.9	137.2	1.5	38.9	
	B3LYP-GD3BJ	-18.6	95.1	101.5	-6.5	-58.7	84.4
		-17.6	106.0	110.2	0.2	59.8	
	M06-2X	21.4	-119.6	87.9	-4.0	69.7	-74.2
		-16.2	-118.1	91.0	-0.8	-69.8	
$[C_4mim:PF_6:C_6mim]^+$	B3LYP	-10.3	-99.9	136.0	-0.3	38.2	-51.2
		8.6	99.8	132.0	-2.7	-40.0	
	B3LYP-GD3BJ	-18.4	106.5	110.5	0.4	59.1	93.4
		-17.2	106.0	109.4	0.0	59.9	
	M06-2X	17.1	118.3	90.9	-0.7	69.7	75.4
		21.4	-114.2	88.5	-4.7	68.6	
$[C_6mim:PF_6:C_8mim]^+$	B3LYP	-11.0	-100.4	135.4	-1.1	38.5	-83.0
		14.2	-102.6	137.5	1.5	-38.7	
	B3LYP-GD3BJ	18.7	-106.2	110.1	1.2	-59.8	65.1
		-17.5	98.3	114.4	0.7	56.6	
	M06-2X	-20.6	111.3	88.0	-4.4	-69.5	-63.1
		21.9	-110.8	88.9	-5.3	67.8	

system	theory	C1′H-F	C2H-F	C1″H-F	C2-F	C2-P
$[C_2mim:PF_6:C_4mim]^+$	B3LYP	2.439	2.193, 2.209	2.407	3.276	3.811
		2.673	2.157, 2.285	2.415	3.273	3.811
	B3LYP-GD3BJ	2.399	2.504, 2.311	2.663	2.908	3.548
		2.573	2.340, 2.322	2.364	2.866	3.577
	M06-2X	2.550	2.563, 2.424	2.727	2.839	3.429
		2.474	2.436, 2.455	2.655	2.809	3.427
$[C_4mim:PF_6:C_6mim]^+$	B3LYP	2.443	2.206, 2.234	2.415	3.181	3.781
		2.462	2.272, 2.212	2.410	3.133	3.760
	B3LYP-GD3BJ	2.523	2.311, 2.358	2.386	3.579	3.579
		2.558	2.311, 2.390	2.390	3.578	3.578
	M06-2X	2.459	2.418, 2.481	2.684	3.429	3.429
		2.515	2.548, 2.430	2.704	3.432	3.432
$[C_6mim:PF_6:C_8mim]^+$	B3LYP	2.479	2.204, 2.245	2.378	3.214	3.790
		2.669	2.146, 2.287	2.411	3.270	3.807
	B3LYP-GD3BJ	2.510	2.294, 2.450	2.448	2.795	3.585
		2.560	2.261, 2.387	2.437	2.889	3.617
	M06-2X	2.496	2.569, 2.416	2.688	2.837	3.429
		2.491	2.551, 2.405	2.685	2.837	3.430

[a]Bond and dihedral angles are given in (°). The optimized structures were determined using the density functional indicated with a 6-311+G(d,p) basis set and are shown in **Figure 6** and **Figures S2-4**. See **Figure S1** for dihedral definitions. [b]First 1-alkyl dihedral angle a1 ≡ ∠C2N1C1′C2′. [c]Binding site dihedral angle defined as **b** ≡ ∠(C2,©,©+CP,P), where © denotes the centroid of the imidazolium ring. [d]Binding orientation dihedral angle defined as **b1** ≡ ∠C1″N3C2P. [e]Relative cation binding orientation dihedral angle defined as **b2** ≡ ∠C1′N1N1C1′.

Table S6. Fitting Parameters of **eqn (3)**, Threshold Dissociation Energies at 0 K, and Entropies of Activation at 1000 K of $[C_{n-2}mim:PF_6:C_nmim]^+$ Clusters Based on Independent Fitting of the Two Primary Dissociation Pathways[a]

system	Ionic Product	E_0(PSL)[b] (eV)	$\Delta S^{\ddagger}$(PSL)[b] (J mol^{-1} K^{-1})	σ[b]	n	E_0[c] (eV)	kinetic shift (eV)
$[C_2mim:PF_6:C_4mim]^+$	$[C_2mim]^+$	1.17 (0.05)	18 (4)	28.0 (1.9)	1.3 (0.1)	2.07 (0.08)	0.90
	$[C_4mim]^+$	1.15 (0.05)	17 (4)	60.2 (2.6)	1.1 (0.1)	2.03 (0.08)	0.88
$[C_4mim:PF_6:C_6mim]^+$	$[C_4mim]^+$	1.14 (0.07)	17 (4)	34.7 (3.0)	1.2 (0.1)	2.31 (0.09)	1.16
	$[C_6mim]^+$	1.15 (0.06)	24 (4)	44.0 (3.1)	1.3 (0.1)	2.31 (0.09)	1.17
$[C_6mim:PF_6:C_8mim]^+$	$[C_6mim]^+$	1.05 (0.05)	9 (4)	35.9 (1.5)	1.4 (0.1)	2.63 (0.10)	1.57
	$[C_8mim]^+$	1.02 (0.06)	5 (4)	39.9 (1.4)	1.4 (0.1)	2.57 (0.10)	1.55

[a]Present results, uncertainties are listed in parentheses. [b]Average values for loose PSL TS. [c]No RRKM analysis.

Table S7. Vibrational Frequencies and Average Vibrational Energies of the $[C_{n-2}mim:PF_6:C_nmim]^+$ Clusters, $[C_nmim]^+$ Cations, and ($C_nmim:PF_6$) Ion Pairs[a]

system	E_{int}, eV[b]	vibrational frequencies (cm^{-1})
$[C_2mim:PF_6:C_4mim]^+$	0.79 (0.06)	5, 9, 12, 18, 23, 30, 33, 39, 41, 50, 58, 63, 74, 79, 88, 106, 109, 119, 120, 146, 202, 209, 235, 242, 247, 278, 282, 295, 298(2), 322, 381, 406, 426, 438, 439, 441, 446, 524(2), 528, 534, 540, 595, 629, 636(2), 666, 668, 685, 700, 735, 745, 748(2), 804, 806, 810, 828, 833, 867, 868, 901, 908, 917, 951, 964, 1012, 1037, 1038, 1044, 1045, 1056, 1103, 1107, 1108, 1121(2), 1129, 1139, 1153, 1156(2), 1176, 1177, 1239, 1272, 1297, 1302, 1312, 1321, 1340, 1347, 1349, 1383, 1390, 1401, 1414(2), 1421, 1426, 1445, 1449, 1463, 1464, 1492, 1493, 1494, 1495, 1497(2), 1502, 1504, 1511, 1512, 1513, 1516, 1595(2), 1603, 1605, 3012, 3022, 3028, 3042, 3043, 3065(2), 3066, 3078(2), 3091, 3099, 3107, 3118, 3128, 3138, 3142(2), 3168(2), 3275, 3276, 3284, 3286, 3294(2)
$[C_4mim:PF_6:C_6mim]^+$	0.94 (0.07)	5, 8, 10, 16, 19, 21, 30, 37, 38, 43, 49, 51, 59, 65, 72, 76, 79, 91, 102, 111, 113, 121, 123, 141, 146, 205, 219, 240, 243, 246, 249, 282(2), 286, 295(2), 299, 317, 409, 412, 435, 438(2), 441, 446, 450, 523, 525, 528, 534, 540, 628(2), 637, 638, 669, 670, 684, 735, 739, 742, 744, 747, 748, 751, 802, 804, 809, 829, 831, 866, 867, 897, 900, 903, 907, 917, 949, 1003, 1006, 1013, 1037, 1038(2), 1043, 1045, 1051, 1058, 1066, 1108(2), 1121, 1122, 1130, 1136, 1154, 1155, 1156, 1157, 1175, 1177, 1220, 1238, 1263, 1272, 1295, 1301, 1302, 1320, 1322, 1327, 1335, 1336, 1339, 1350(2), 1381, 1386, 1399, 1400, 1403, 1416, 1417, 1418, 1422, 1447, 1448, 1464(2), 1487, 1489, 1491, 1494, 1495, 1496, 1497, 1501, 1502, 1503, 1506, 1511(2), 1512, 1517(2), 1595, 1596, 1604, 1605, 2999, 3004, 3012, 3013, 3018, 3021(2), 3024, 3029, 3032, 3038, 3048, 3061, 3063, 3065(2), 3074(2), 3084, 3090, 3093, 3101, 3129(2), 3142(2), 3168, 3169, 3276(2), 3288, 3289, 3294, 3295
$[C_6mim:PF_6:C_8mim]^+$	1.09 (0.08)	1, 8, 10, 11, 16, 18, 29, 32, 36, 37, 41, 44, 49, 53, 58, 60, 66, 77, 83, 94, 97, 103, 108, 109, 115, 127, 140, 147, 150, 155, 176, 200, 217, 239, 244(2), 245, 281, 283, 287, 295, 296, 299, 312, 376, 413, 418, 438(2), 441, 446, 448, 451, 494, 523, 524, 527, 533, 540, 628, 630, 637, 638, 671, 672, 685, 733, 735, 738, 740, 741, 748(2), 752, 759, 802, 803, 809, 828, 832, 866, 867, 873, 898(2), 900, 905, 909, 956, 994, 1003, 1006, 1007, 1032, 1037(2), 1038, 1040, 1044, 1047, 1051, 1061, 1064, 1066, 1072, 1107(2), 1122(2), 1136, 1139, 1155(2), 1156, 1160, 1176, 1177, 1213, 1220, 1246, 1253, 1263, 1273, 1289, 1296, 1302, 1308, 1322, 1327(2), 1329, 1335, 1338, 1339, 1341, 1343, 1350, 1351, 1378, 1381, 1396, 1398, 1402(2), 1404, 1415, 1417(2), 1419, 1445, 1448, 1463, 1464, 1486, 1487, 1488, 1489, 1491, 1492, 1494, 1497(2), 1498, 1501(2), 1502, 1505, 1510, 1511(2), 1512, 1517, 1518, 1596(2), 1604(2), 2994, 2997, 2999, 3001, 3004, 3006, 3011(2), 3012, 3018, 3019, 3020, 3021, 3023, 3024, 3032(2), 3043, 3048, 3055, 3063, 3065(3), 3073, 3079, 3080, 3084, 3088, 3093, 3127, 3128, 3142(2), 3168, 3170, 3276(2), 3284, 3288, 3295(2)
$[C_2mim]^+$	0.19 (0.02)	46, 69, 135, 209, 233, 292, 378, 425, 592, 633, 660, 698, 753, 803, 834, 881, 962, 1036, 1043, 1099, 1102, 1124, 1136, 1150, 1175, 1270, 1311, 1343, 1385, 1411, 1428, 1437, 1461, 1484, 1491, 1494, 1509, 1510, 1595, 1604, 3046, 3070, 3079, 3110, 3122, 3134, 3150, 3165, 3274, 3278, 3292
$[C_4mim]^+$	0.27 (0.02)	28, 65, 69, 83, 112, 199, 237, 247, 273, 318, 407, 434, 626, 632, 664, 733, 741, 752, 801, 834, 879, 916, 946, 1010, 1037, 1042, 1054, 1100, 1125, 1128, 1147, 1150, 1175, 1234, 1295, 1299, 1318, 1336, 1345, 1381, 1395, 1412, 1424, 1436, 1460, 1484, 1489, 1492, 1502(2), 1510, 1515, 1594, 1603, 3015, 3025, 3032, 3041, 3065, 3069, 3072, 3094, 3108, 3121, 3149, 3165, 3274, 3279, 3292

Table S7. Vibrational Frequencies and Average Vibrational Energies of the $[C_{n-2}mim:PF_6:C_nmim]^+$ Clusters, $[C_nmim]^+$ Cations, and ($C_nmim:PF_6$) Ion Pairs[a]

system	E_{int}, eV[b]	vibrational frequencies (cm^{-1})
$[C_6mim]^+$	0.34 (0.03)	28, 49, 52, 63, 76, 124, 131, 147, 214, 238, 245, 278, 294, 408, 437, 449, 626, 631, 666, 736, 737, 750, 754, 802, 833, 881, 897, 901, 1001, 1007, 1035, 1037, 1041, 1046, 1062, 1099, 1125, 1135, 1149, 1154, 1174, 1219, 1262, 1272, 1303, 1320, 1326, 1336, 1340, 1344, 1378, 1394, 1401, 1412, 1420, 1436, 1460, 1484, 1488, 1489, 1493, 1500, 1502, 1510(2), 1510, 1517, 1595, 1603, 3001, 3006, 3015, 3022, 3024, 3026, 3035, 3051, 3067, 3068, 3072, 3086, 3098, 3122, 3148, 3164, 3274, 3277, 3291
$[C_8mim]^+$	0.42 (0.03)	20, 38, 40, 53, 70, 93, 96, 107, 149, 156, 175, 193, 242(2), 279, 311, 374, 416, 448, 492, 626, 631, 666, 734, 736, 738, 752, 757, 801, 833, 872, 880, 900, 955, 994, 1004, 1032, 1036, 1038, 1044, 1059, 1064, 1072, 1100, 1125, 1138, 1148, 1155, 1172, 1211, 1245, 1251, 1286, 1294, 1306, 1322, 1329, 1338, 1340, 1342, 1345, 1378, 1392, 1402, 1403, 1412, 1419, 1435, 1461, 1484, 1486, 1487, 1491, 1492, 1497, 1501, 1505, 1511, 1512, 1517, 1594, 1603, 2996, 2999, 3004, 3009, 3014(2), 3022(2), 3025, 3032, 3044, 3055, 3068(2), 3071, 3083, 3091, 3120, 3148, 3164, 3275, 3277, 3292
($C_2mim:PF_6$)	0.42 (0.03)	3, 32, 36, 57, 69, 81, 99, 117, 166, 214, 238, 285, 293, 297, 303, 386, 426, 438, 442, 444, 511, 522, 526, 528(2), 596, 635, 669, 671, 705, 737, 806, 828, 832, 846, 857, 928, 965, 1039, 1047, 1104, 1109, 1120, 1138, 1157, 1179, 1272, 1313, 1352, 1393, 1413, 1424, 1455, 1464, 1493, 1497, 1501, 1510, 1514, 1596, 1605, 3037, 3060, 3079, 3102, 3113, 3139(2), 3165, 3277, 3279, 3295
($C_4mim:PF_6$)	0.49 (0.04)	11, 16, 34, 53, 60, 64, 76, 87, 112, 118, 139, 213, 241, 251, 284, 288, 293, 297, 318, 418, 431, 438, 441, 445, 513, 521, 527(2), 528, 628, 639, 670, 672, 735, 742, 747, 803, 828, 832, 844, 854, 912, 926, 949, 1015, 1039, 1046, 1062, 1109, 1120, 1131, 1153, 1158, 1178, 1238, 1294, 1301, 1320, 1336, 1355, 1389, 1402, 1415, 1421, 1455, 1465, 1491, 1494, 1501, 1503, 1506, 1511, 1517, 1596, 1604, 3010, 3017, 3024, 3039, 3058, 3060, 3074, 3086, 3095, 3130, 3139, 3166, 3277, 3280, 3295
($C_6mim:PF_6$)	0.57 (0.04)	18, 19, 33, 40, 48, 56, 67, 74, 91, 99, 119, 129, 146, 150, 226, 244, 246, 284, 286, 293, 296, 299, 410, 438, 439, 441, 443, 457, 514, 521, 527(2), 528, 629, 642, 671, 674, 735, 738, 741, 752, 802, 824, 832, 843, 858, 897, 900, 924, 1003, 1008, 1036, 1039, 1044, 1051, 1065, 1108, 1121, 1136, 1156, 1161, 1177, 1222, 1264, 1274, 1303, 1324, 1327, 1337, 1342, 1352, 1377, 1398, 1404, 1415, 1416, 1450, 1463, 1487, 1489, 1494, 1499, 1500, 1501, 1509, 1510, 1515, 1596, 1604, 2994, 2997, 3005, 3014, 3019, 3028, 3037, 3055, 3060, 3060, 3081, 3086, 3093, 3132, 3138, 3165, 3277, 3282, 3296
($C_8mim:PF_6$)	0.64 (0.05)	12, 14, 30, 33, 40, 47, 59, 63, 75, 91, 98, 106, 113, 128, 148, 155, 179, 212, 245, 247, 285, 287, 293, 295, 315, 379, 420, 438, 441, 443, 450, 496, 515, 521, 526, 527, 528, 629, 641, 671, 673, 732, 737, 738, 741, 758, 803, 824, 832, 844, 858, 874, 898, 917, 958, 995, 1006, 1034, 1038, 1041, 1048, 1062, 1066, 1073, 1108, 1121, 1139, 1156, 1163, 1175, 1214, 1247, 1254, 1288, 1297, 1307, 1328, 1332, 1339, 1343, 1345, 1354, 1378, 1397, 1403, 1407, 1415, 1417, 1450, 1463, 1485, 1486, 1490, 1493, 1497, 1500, 1501, 1504, 1509, 1511, 1516, 1595, 1604, 2992, 2994, 2996, 3001, 3006, 3014, 3015, 3018, 3025, 3035, 3045, 3058, 3059, 3060, 3079, 3083, 3095, 3132, 3138, 3165, 3278, 3281, 3296

[a] Determined at the B3LYP/6-311+G(d,p) level of theory and with frequencies scaled by 0.9887. Degeneracies are listed in parentheses. [b]Uncertainties are listed in parentheses.

Table S8. Rotational Constants (in cm^{-1}) of $[C_{n-2}mim:PF_6:C_nmim]^+$ Clusters and the Corresponding PSL Transition States

system	ionic product	energized molecule		transition state		
		1-D[a]	2-D[b]	1-D[c]	2-D[c]	2-D[d]
$[C_2mim:PF_6:C_4mim]^+$	$[C_2mim]^+$	0.01040	0.00288	0.178, 0.0165	0.0393, 0.0075	0.0009
	$[C_4mim]^+$	0.01040	0.00288	0.132, 0.0273	0.0167, 0.0106	0.0009
$[C_4mim:PF_6:C_6mim]^+$	$[C_4mim]^+$	0.00503	0.00188	0.132, 0.0121	0.0167, 0.00604	0.0007
	$[C_6mim]^+$	0.00503	0.00188	0.110, 0.0165	0.00831, 0.00748	0.0007
$[C_6mim:PF_6:C_8mim]^+$	$[C_6mim]^+$	0.00323	0.00144	0.110, 0.0118	0.00831, 0.00361	0.0005
	$[C_8mim]^+$	0.00323	0.00144	0.096, 0.0121	0.00470, 0.00604	0.0005

[a]Active external. [b]Inactive external. [c]Rotational constants of the transition state treated as free internal rotors. [d]Two-dimensional rotational constants of the transition state at threshold, treated variationally and statistically.

FIGURE CAPTIONS

Figure S1. Nomenclature employed in this work to describe the stable conformations predicted for the $[C_n\text{mim}]^+$ cations, ($C_n$mim:PF_6) ion pairs, and $[2C_n\text{mim:}PF_6]^+$ and $[C_{n-2}\text{mim:}PF_6\text{:}C_n\text{mim}]^+$ clusters.

Figure S2. B3LYP/6-311+G(d,p) optimized geometries of the ground conformers of the $[C_n\text{mim}]^+$ cations and $[PF_6]^-$ anion. Noncovalent interaction maps at an isosurface of 0.20 a.u. of the reduced electron density gradients determined using a 6-311+G(2d,2p) basis set have been superimposed on the optimized structures.

Figure S3. B3LYP/6-311+G(d,p) optimized geometries of the ground conformers of the ($C_n$mim:PF_6) ion pairs. Noncovalent interaction maps at an isosurface of 0.20 a.u. of the reduced electron density gradients determined using a 6-311+G(2d,2p) basis set have been superimposed on the optimized structures.

Figure S4. B3LYP/6-311+G(d,p) and M06-2X/6-311+G(d,p) optimized geometries of the ground conformers of the $[C_{n-2}\text{mim:}PF_6\text{:}C_n\text{mim}]^+$ clusters. Noncovalent interaction maps at an isosurface of 0.20 a.u. of the reduced electron density gradients determined using the 6-311+G(2d,2p) basis set have been superimposed on the optimized structures.

Figure S5. B3LYP/6-311+G(d,p) optimized geometries of the ground and select stable conformers of the $[C_2\text{mim:}PF_6\text{:}C_4\text{mim}]^+$ cluster. Conformer designations along with the B3LYP/6-311+G(2d,2p), B3LYP-GD3BJ/6-311+G(2d,2p) and M06-2X/6-311+G(2d,2p) relative Gibbs energies at 298 K (in kJ/mol) are also listed. The [g_;**g_g+Fg_F**;g_t2] structure is optimized at the M06-2X/6-311+G(d,p) level of theory. Conformers not determined upon M06-2X or B3LYP-GD3BJ re-optimization of the B3LYP optimized structures (due to significant structural rearrangement) are indicated with a dash.

Figure S6. B3LYP/6-311+G(d,p) optimized geometries of the ground and select stable conformers of the $[C_4\text{mim:}PF_6\text{:}C_6\text{mim}]^+$ cluster. Conformer designations along with the B3LYP/6-311+G(2d,2p), B3LYP-GD3BJ/6-311+G(2d,2p) and M06-2X/6-311+G(2d,2p) relative Gibbs energies at 298 K (in kJ/mol) are also listed. The $[g_+t_2;\mathbf{g_+g_+Fg_+F};g_+t_4]^+$ and $[g_+t_2;\mathbf{g_+g_+Fg_+F};g_-t_4]^+$ conformers are optimized using B3LYP-GD3BJ and M06-2X respectively. Conformers not determined upon M06-2X or B3LYP-GD3BJ re-optimization of the B3LYP optimized structures (due to significant structural rearrangement) are indicated with a dash.

Figure S7. B3LYP/6-311+G(d,p) optimized geometries of the ground and select stable conformers of the $[C_6\text{mim:}PF_6\text{:}C_8\text{mim}]^+$ cluster. Conformer designations along with the B3LYP/6-311+G(2d,2p), B3LYP-GD3BJ/6-311+G(2d,2p) and M06-2X/6-311+G(2d,2p) relative Gibbs energies at 298 K (in kJ/mol) are also listed. The $[g_-t_4;\mathbf{g_+g_Fg_+F};g_+t_6]^+$ and $[g_+t_4;\mathbf{g_g_Fg_+F};g_-t_6]^+$ conformers are optimized using B3LYP-GD3BJ and M06-2X respectively. Conformers not determined upon M06-2X or B3LYP-GD3BJ re-optimization of the B3LYP optimized structures (due to significant structural rearrangement) are indicated with a dash.

Figure S8. Electrostatic potential maps of the B3LYP/6-311+G(d,p) and M06-2X/6-311+G(d,p) ground conformers of the $[C_{n-2}mim:PF_6:C_nmim]^+$ clusters. The ESP maps are shown at an isosurface of 0.01 a.u. of the total B3LYP/6-311+G(2d,2p) SCF electron density. The Mülliken charges on the hydrogen atoms of the cations and fluorine atoms of the anion are labeled. The most electropositive regions are color-coded in blue and occur at the hydrogen atoms of the 3-methylimidazolium moiety, with the C2 hydrogen atom displaying the greatest Mülliken charge. The most electronegative regions are color-coded in red, and occur at the fluorine atoms of the anion. Regions of intermediate ESP are shown in green and yellow and become more prevalent as the size of the 1-alkyl substituent increases.

Figure S9. Comparison of the B3LYP, B3LYP-GD3BJ, and M06-2X computed 0 K BDEs versus measured threshold dissociation energies of the $[C_{n-2}mim:PF_6:C_nmim]^+$ clusters for n = 4, 6, and 8 (in kJ/mol). All theoretical values include ZPE and BSSE corrections. The $[C_nmim]^+$ and $[C_{n-2}mim]^+$ primary product cations are indicated with closed and open symbols, respectively. The n–2:n values of each cluster are indicated. The diagonal lines indicate values for which the calculated and measured values are equal.

Figure S10. Comparison of the B3LYP, B3LYP-GD3BJ, and M06-2X computed relative BDEs of the $[C_{n-2}mim:PF_6:C_nmim]^+$ clusters (for n = 4, 6 and 8) and relative IPEs of the $(C_nmim:PF_6)$ ion pairs (for n = 2, 4, 6, and 8) vs. experimentally determined 0 K ΔBDEs of the $[C_{n-2}mim:PF_6:C_nmim]^+$ clusters (for n = 4, 6 and 8). All theoretical values include ZPE and BSSE corrections. The ΔIPEs and ΔBDEs are indicated with open and closed symbols, respectively. The n–2:n values of each cluster are indicated. The diagonal lines indicate values for which the calculated and measured values are equal.

Figure S11. Comparison of the B3LYP, B3LYP-GD3BJ, and M06-2X computed vs. TCID measured 0 K BDEs of the $[2C_nmim:PF_6]^+$ clusters for n = 2, 4, 6, and 8 (in kJ/mol). All theoretical values include ZPE and BSSE corrections. Values derived from direct TCID measurements (taken from reference 1) and those determined from regression analyses using the direct and competitive TCID measurements are indicated with open and closed symbols, respectively. The diagonal lines indicate values for which the calculated and measured values are equal.

REFERENCES

1. H. A. Roy and M. T. Rodgers, *Phys. Chem. Chem. Phys.*, 2021, **23**, 13405-13418.

Figure S1.

$[C_n mim]^+$ Nomenclature

$[a1a2\ldots an\text{-}1]^+$

$[C_2mim]^+ = [a1]^+$
$[C_4mim]^+ = [a1a2a3]^+$
$[C_6mim]^+ = [a1a2a3a4a5]^+$
$[C_8mim]^+ = [a1a2a3a4a5a6a7]^+$

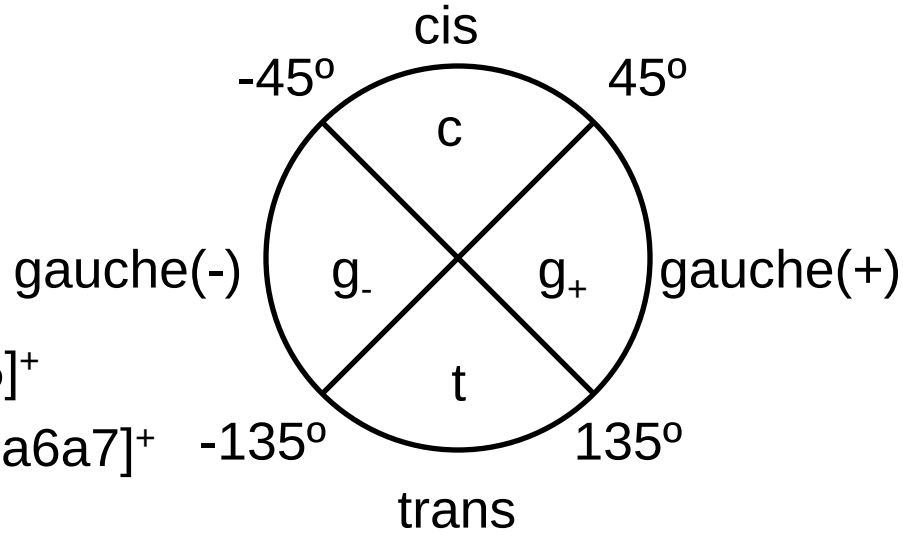

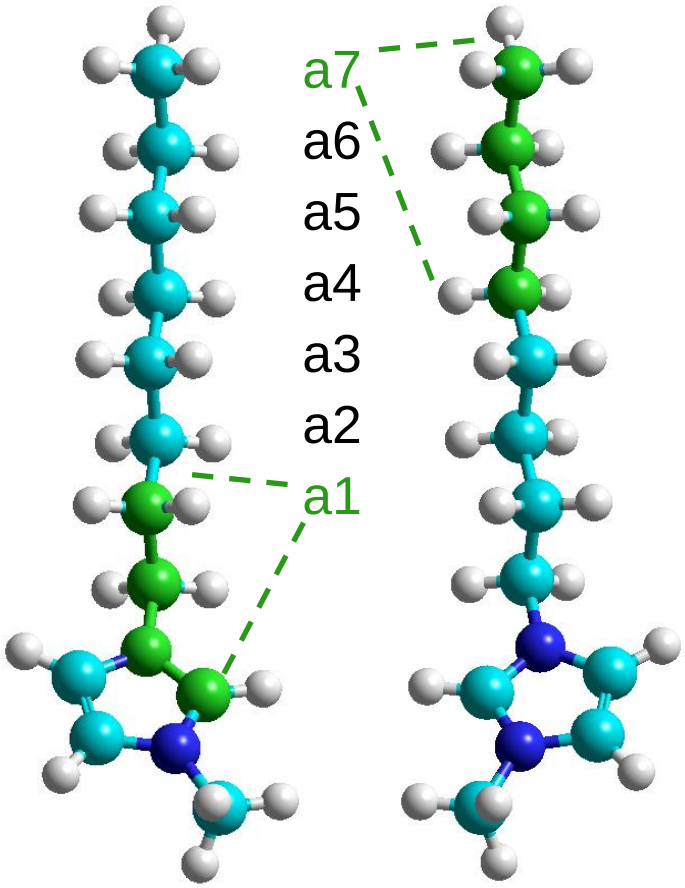

$[g_-ttttt]^+$ $[g_-t_6]^+$ $[g_+ttttt]^+$ $[g_+t_6]^+$

$[C_8mim]^+$

Dihedral Angle Classification

1-Alkyl Dihedral Angles

a1 = ∠C2N1C1′C2′
a2 = ∠N1C1′C2′C3′
a3 = ∠C1′C2′C3′C4′
a4 = ∠C2′C3′C4′C5′
a5 = ∠C3′C4′C5′C6′
a6 = ∠C4′C5′C6′C7′
a7 = ∠C5′C6′C7′C8′

Figure S1.

Binding Site (BS) Nomenclature

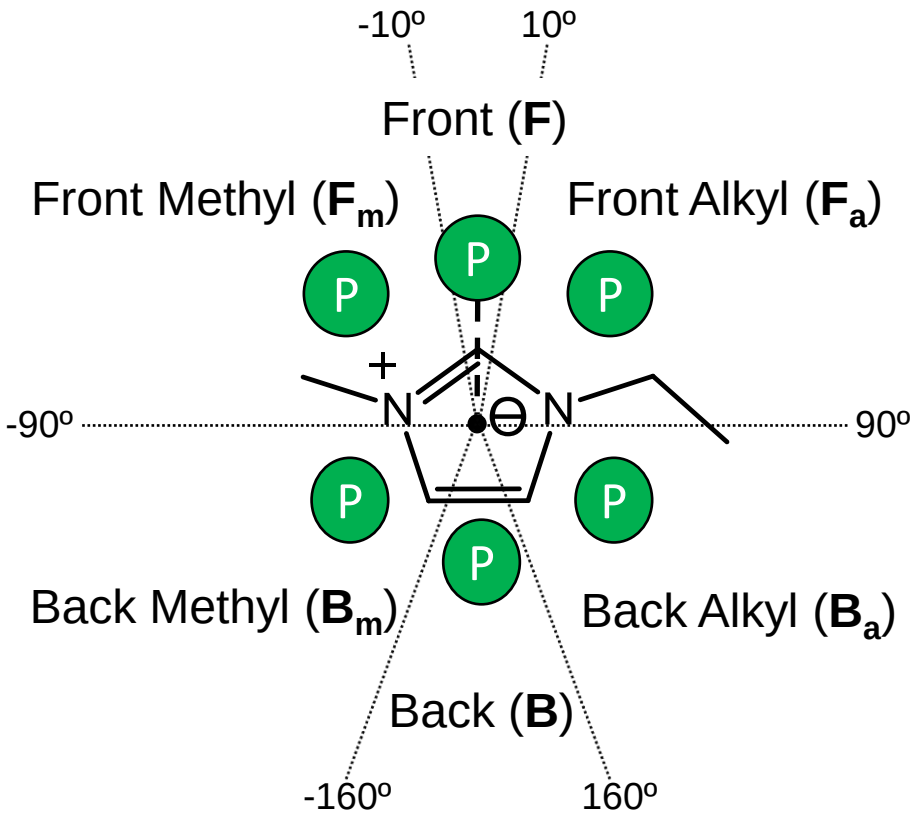

The **binding site** (**BS**) designation is readily described by the dihedral angle **b** = ∠(C2,©,©+CP,P), where © denotes the centroid of the imidazolium ring (N1C2N3C4C5) and CP denotes the cross product of the vectors that describe the C2-N1 and C2-N3 bonds, i.e., CP = $\overrightarrow{(C2\text{-}N1)}x\overrightarrow{(C2\text{-}N3)}$. The range of angles that define BS designations are shown in the figure above and the bar below.

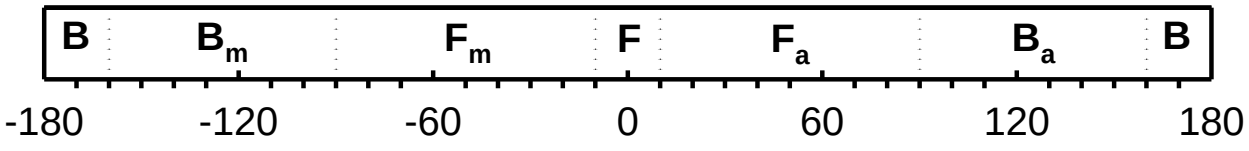

b (Binding Site Dihedral Angle, deg)

Figure S1.

Binding Site (BS) Nomenclature

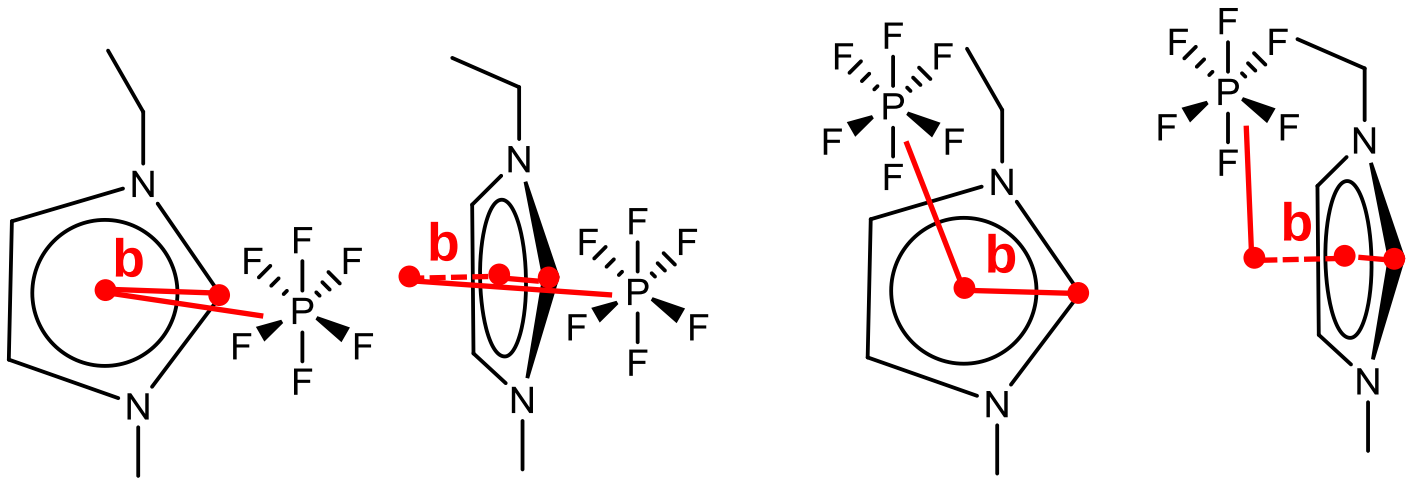

Front Binding (**F**) Back Alkyl Binding ($\mathbf{B_a}$)

The **binding site** (**BS**) designation is readily described by the dihedral angle **b** = ∠(C2,©,©+CP,P), where © denotes the centroid of the imidazolium ring (N1C2N3C4C5) and CP denotes the cross product of the vectors that describe the C2-N1 and C2-N3 bonds, i.e., CP = $\overrightarrow{(C2\text{-}N1)}x\overrightarrow{(C2\text{-}N3)}$. The range of angles that define BS designations are shown in the figure above and the bar below.

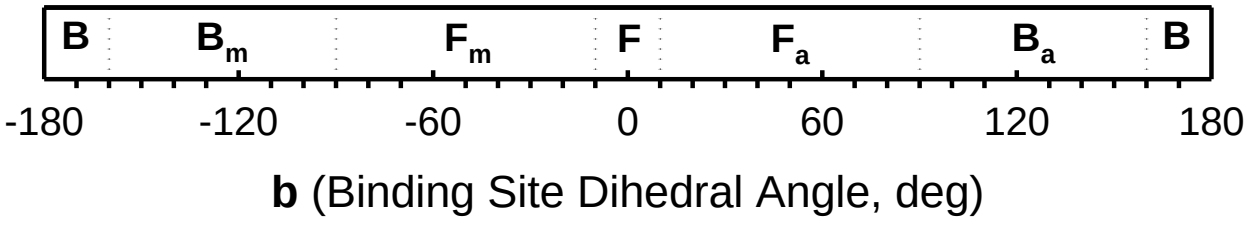

Figure S1.

($C_n$mim:PF_6) Nomenclature

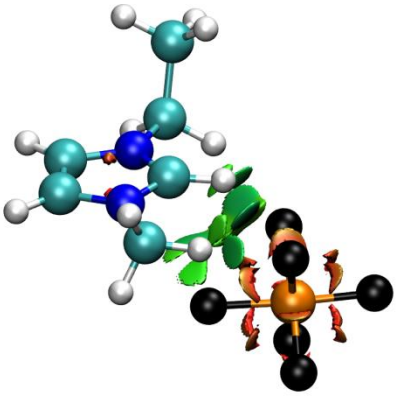

(C_2mim:PF_6)

(**g_+F;**g_-)

(**Binding Site**;Alkyl)

(**b1BS**;a1…an)

b1 = ∠C1″N3C2P

[C_{n-2}mim:PF_6:$C_n$mim]$^+$ Nomenclature

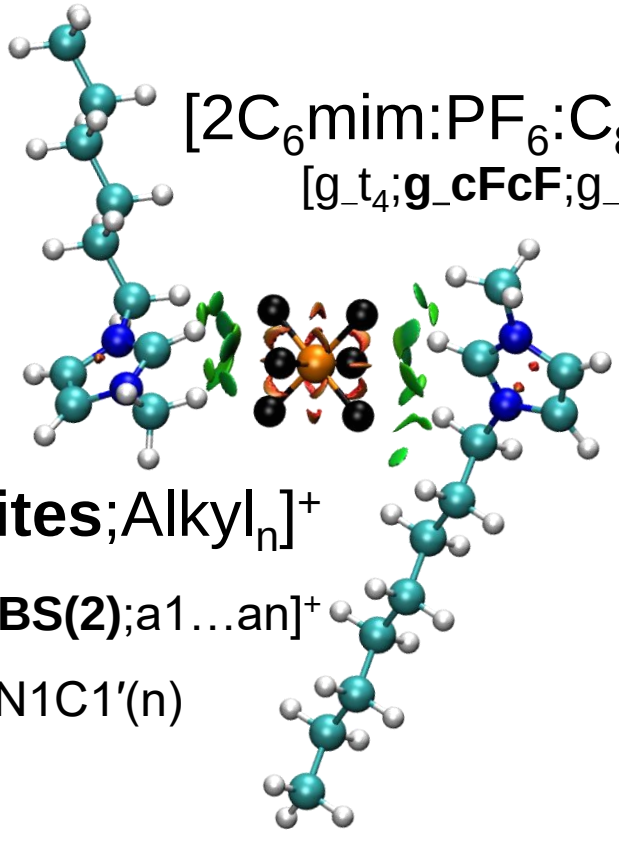

[$2C_6$mim:PF_6:C_8mim]$^+$

[g_t_4;**g_cFcF**;g_t_6]$^+$

[$Alkyl_{n-2}$;**BindingSites**;$Alkyl_n$]$^+$

[a1…an-2;**b2b1BS(1)b1BS(2)**;a1…an]$^+$

b2 = ∠C1′N1(n-2)N1C1′(n)

Figure S2.

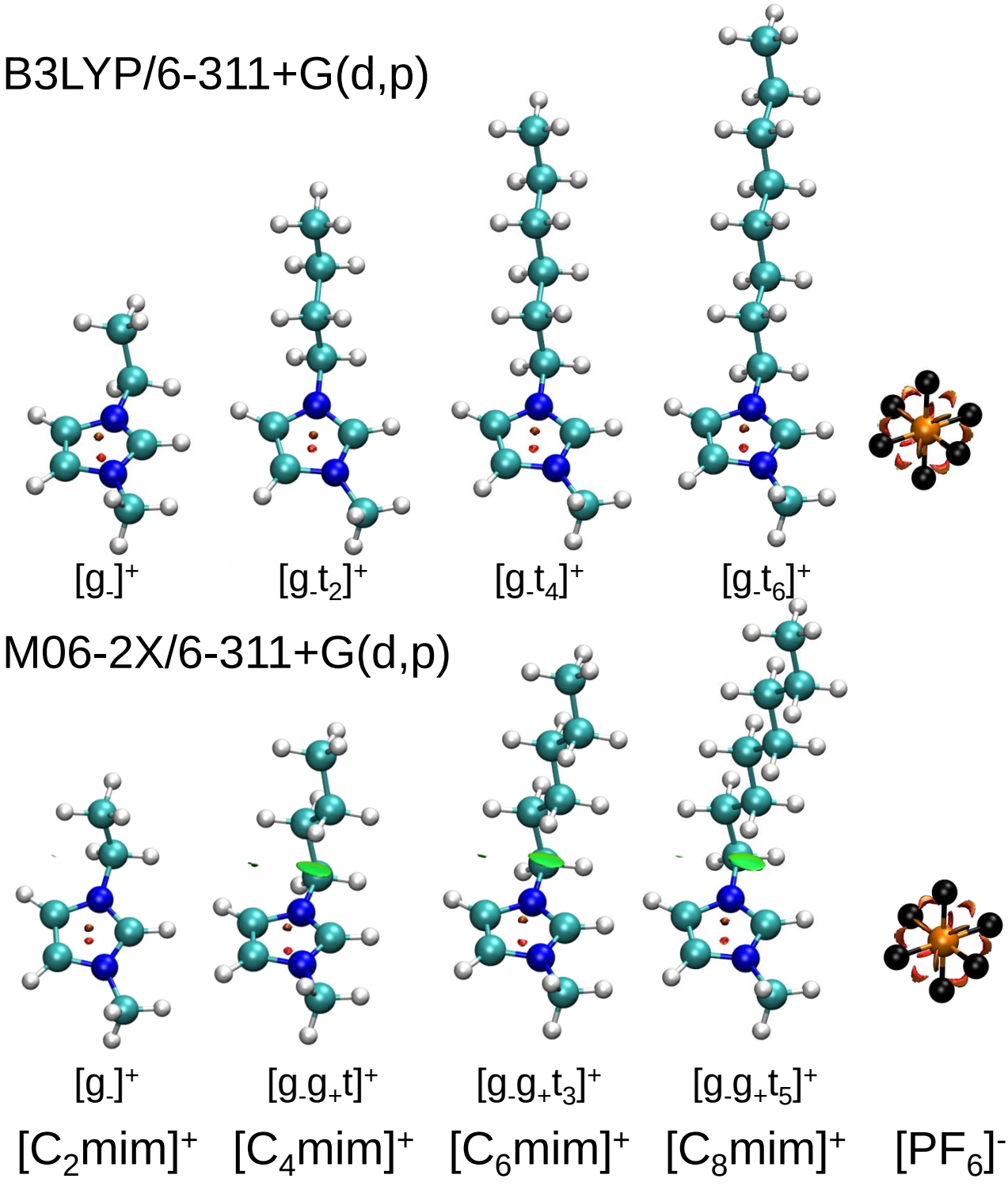
B3LYP/6-311+G(d,p)
[g-]+
[g-t2]+
[g-t4]+
[g-t6]+
M06-2X/6-311+G(d,p)
[g-]+
[g-g+t]+
[g-g+t3]+
[g-g+t5]+
[C2mim]+
[C4mim]+
[C6mim]+
[C8mim]+
[PF6]-

Figure S3.

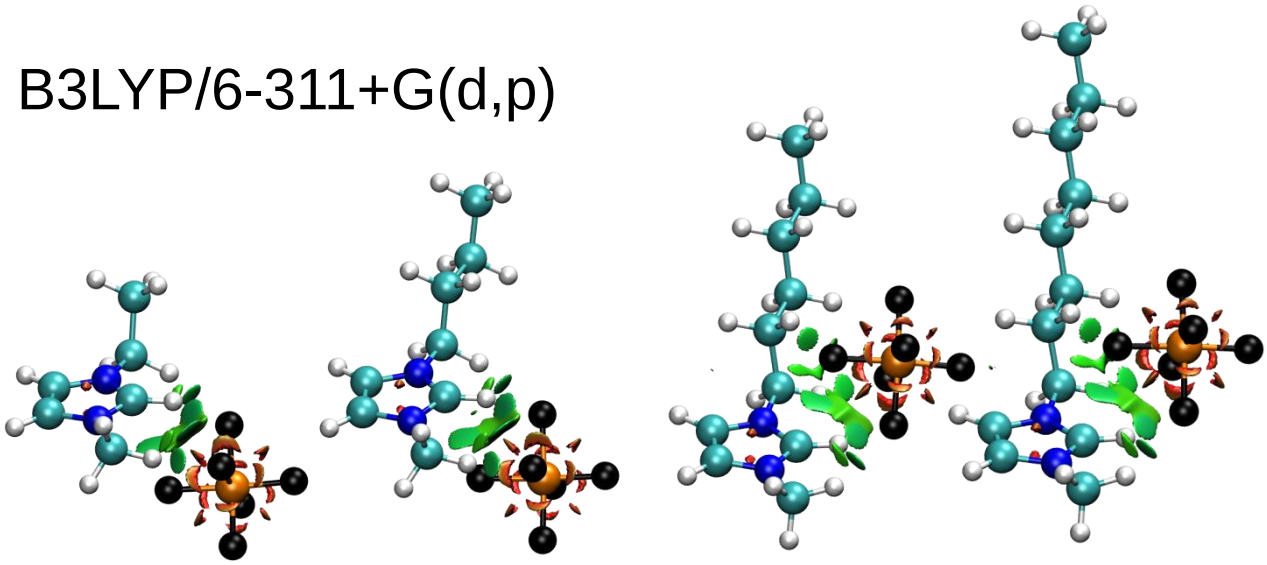
B3LYP/6-311+G(d,p)
(g+F;g-) (g+F;g-t2) (g-F;g-t4) (g-F;g-t6)
(C2mim:PF6) (C4mim:PF6) (C6mim:PF6) (C8mim:PF6)

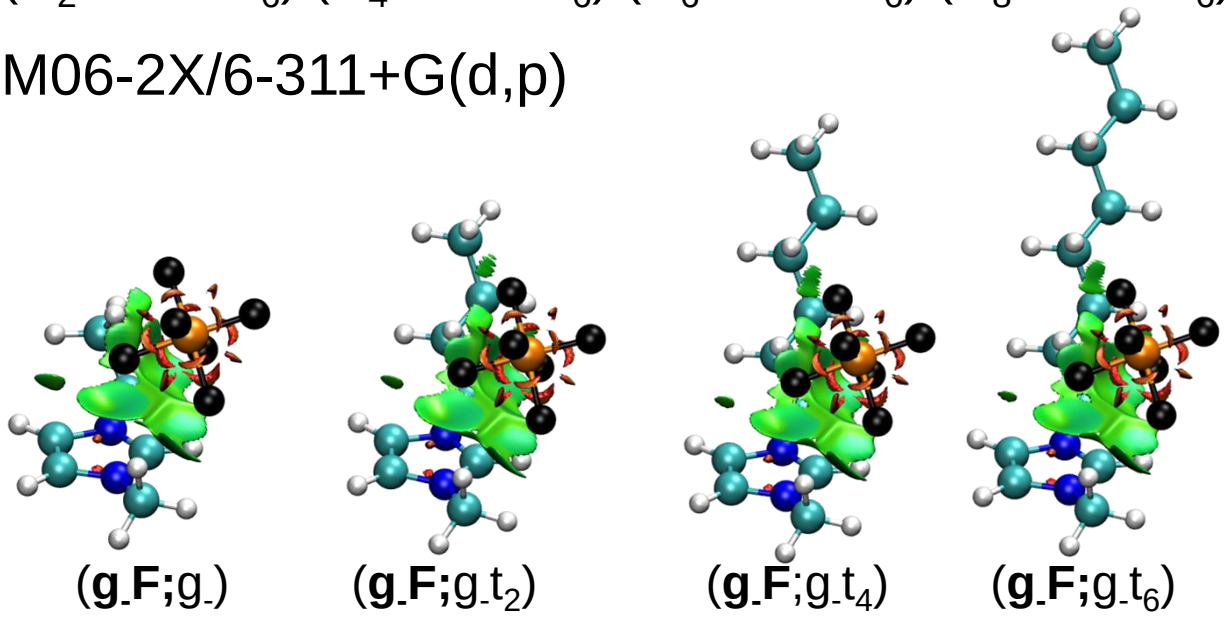
M06-2X/6-311+G(d,p)
(g-F;g-) (g-F;g-t2) (g-F;g-t4) (g-F;g-t6)

Figure S4.

B3LYP/6-311+G(d,p)

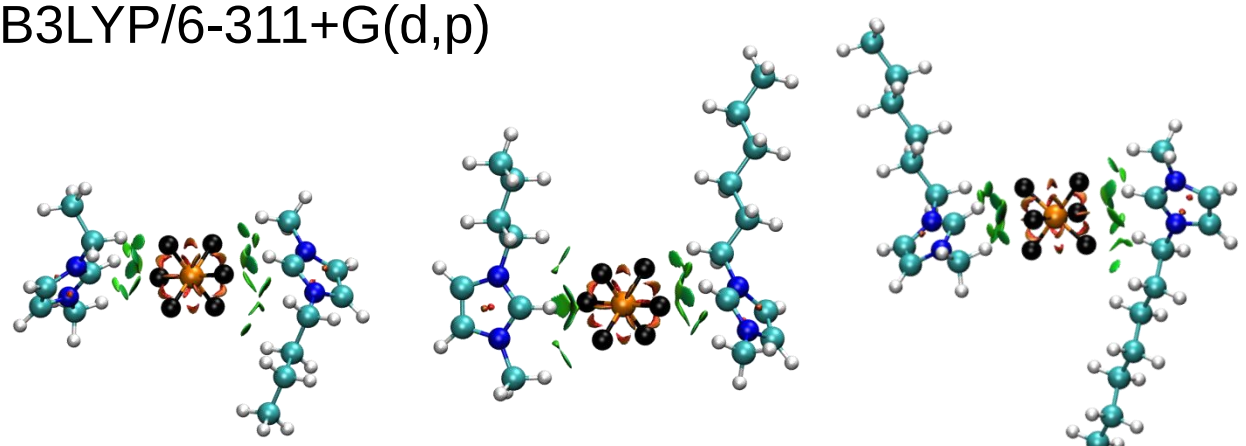

$[g_{-};\mathbf{g_{-}cFcF};g_{-}t_{2}]^{+}$ $[g_{-}t_{2};\mathbf{g_{-}cFcF};g_{+}t_{4}]^{+}$ $[g_{-}t_{4};\mathbf{g_{-}cFcF;}g_{-}t_{6}]^{+}$

$[C_2mim:PF_6:C_4mim]^{+}$ $[C_4mim:PF_6:C_6mim]^{+}$ $[C_6mim:PF_6:C_8mim]^{+}$

$[g_{-};\mathbf{g_{-}g_{+}Fg_{-}F};g_{-}t_{2}]^{+}$ $[g_{+}t_{2};\mathbf{g_{+}g_{+}Fg_{+}F};g_{-}t_{4}]^{+}$ $[g_{+}t_{4};\mathbf{g_{-}g_{-}Fg_{+}F;}g_{-}t_{6}]^{+}$

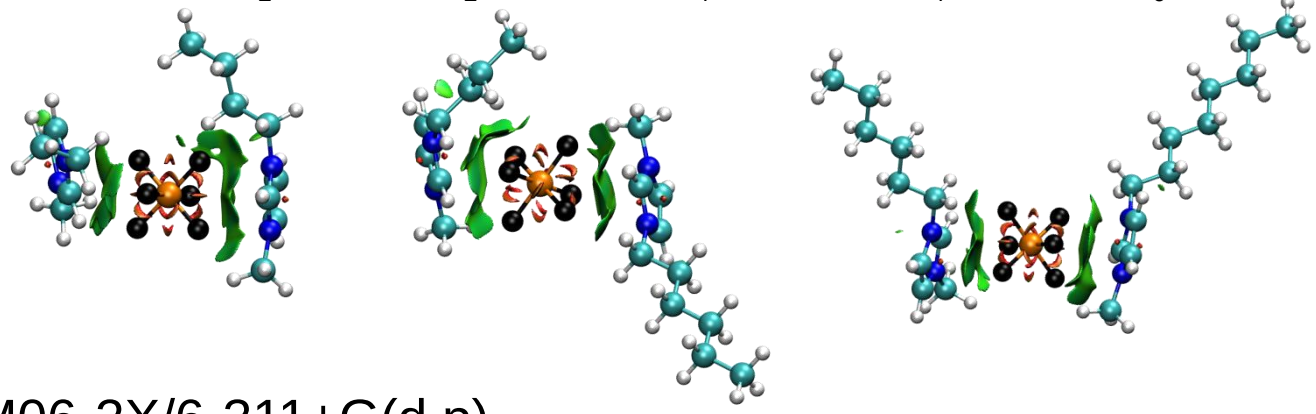

M06-2X/6-311+G(d,p)

Figure S5.

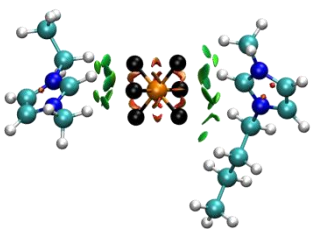

$[g_-;\mathbf{g_-cFcF};g_-t_2]^+$
0.0, -, - kJ/mol

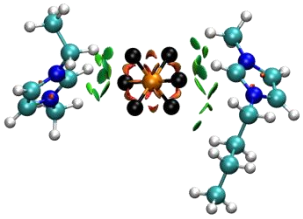

$[g_+;\mathbf{g_+cFcF};g_+t_2]^+$
0.0, -, - kJ/mol

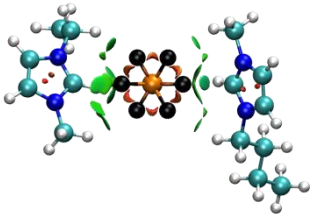

$[g_+;\mathbf{g_-cFcF};g_+t_2]^+$
0.3, -, - kJ/mol

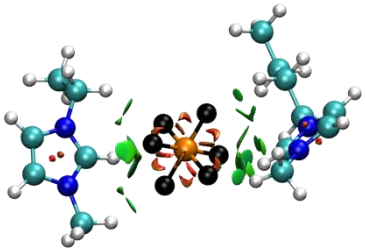

$[g_+;\mathbf{g_-cFcF};g_+t_2]^+$
1.2, -, - kJ/mol

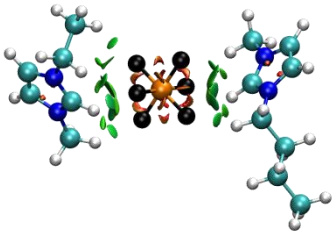

$[g_+;\mathbf{g_+cFcF};g_+t_2]^+$
2.2, -, - kJ/mol

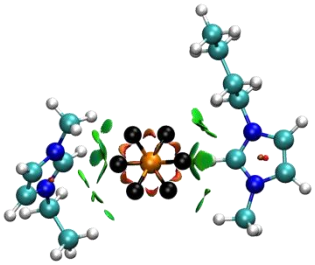

$[g_+;\mathbf{g_+cFcF};g_+t_2]^+2$
2.5, -, - kJ/mol

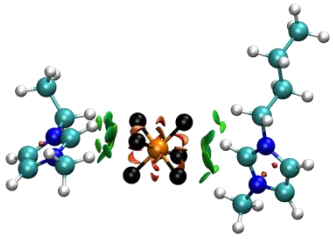

$[g_-;\mathbf{g_+cFcF};g_-t_2]^+$
3.1, -, - kJ/mol

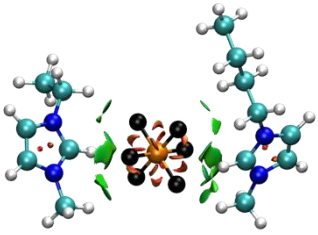

$[g_+;\mathbf{g_+cFcF};g_-t_2]^+$
3.2, -, - kJ/mol

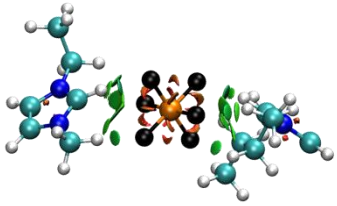

$[g_-;\mathbf{ccFcF};g_-t_2]^+$
3.5, -, - kJ/mol

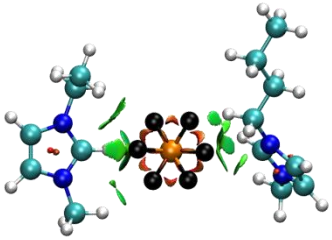

$[g_-;\mathbf{g_+cFcF;}g_-t_2]^+$
3.6, -, - kJ/mol

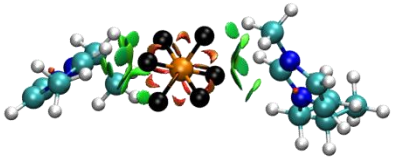

$[g_+;\mathbf{g_-cFcF};g_+t_2]^+$
3.6, -, - kJ/mol

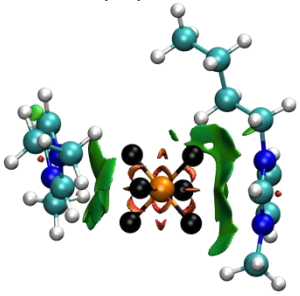

$[g_-;\mathbf{g_-g_+Fg_-F};g_-t_2]^+$
-, 0.0, 0.0, kJ/mol

$[C_2mim{:}PF_6{:}C_4mim]^+$

Figure S6.

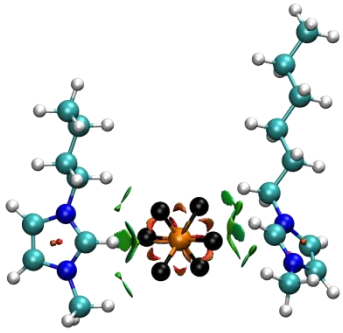

$[g_{-}t_2;\mathbf{g_{-}cFcF};g_{+}t_4]^{+}$
0.0, -, - kJ/mol

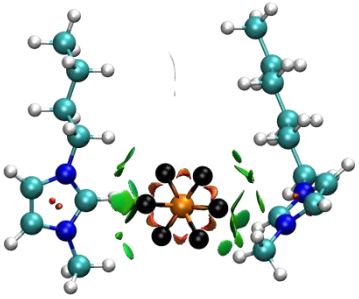

$[g_{+}t_2;\mathbf{g_{-}cFcF};g_{+}t_4]^{+}$
0.0, -, - kJ/mol

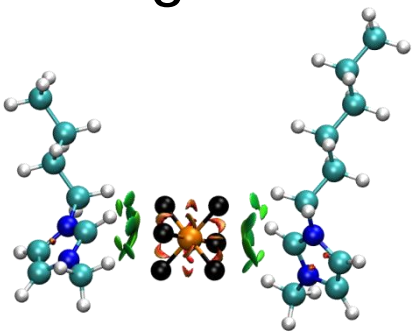

$[g_{-}t_2;\mathbf{g_{+}cFcF};g_{-}t_4]^{+}$
0.5, -, - kJ/mol

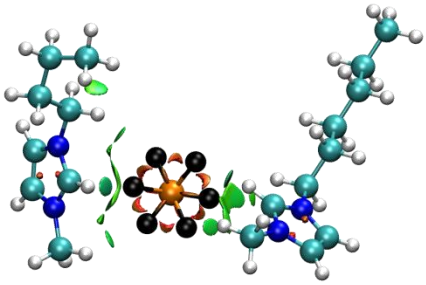

$[g_{-}tg_{-};\mathbf{g_{-}cFcF};g_{+}t_4]^{+}$
0.5, -, - kJ/mol

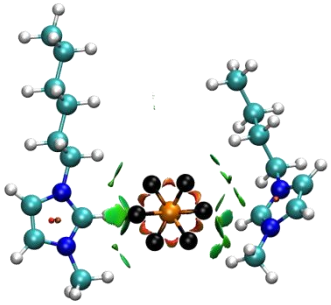

$[g_{+}t_2;\mathbf{ccFcF};g_{+}t_4]^{+}$
1.1, -, - kJ/mol

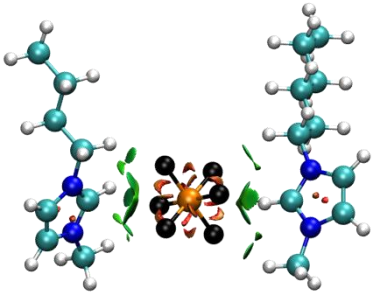

$[g_{+}t_2;\mathbf{g_{-}cFcF};g_{-}t_4]^{+}$
1.2, -, - kJ/mol

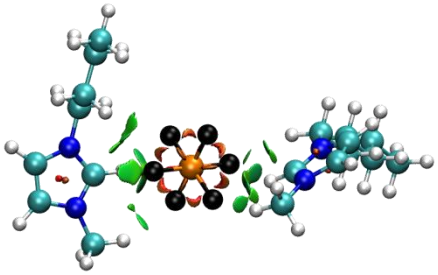

$[g_{-}t_2;\mathbf{g_{-}cFcF};g_{-}t_4]^{+}$
1.3, -, - kJ/mol

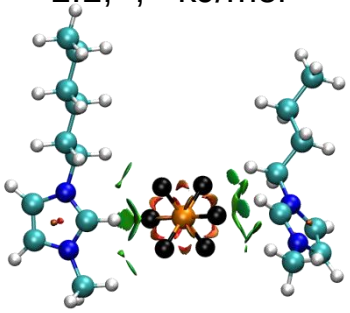

$[g_{+}t_2;\mathbf{g_{-}cFcF};g_{-}t_4]^{+}$
1.4, -, - kJ/mol

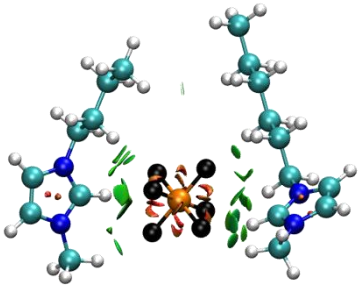

$[g_{-}t_2;\mathbf{g_{-}cFcF};g_{+}t_4]^{+}$
1.6, -, - kJ/mol

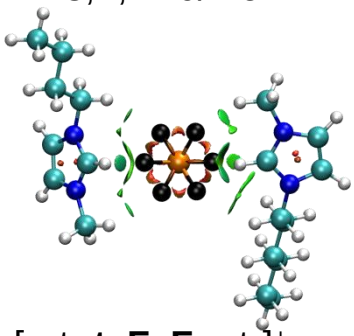

$[g_{-}t_2;\mathbf{tcFcF};g_{+}t_4]^{+}$
1.8, -, - kJ/mol

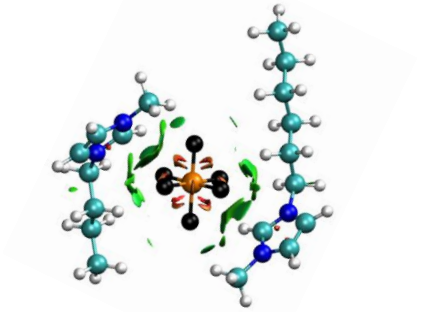

$[g_{+}t_2;\mathbf{g_{+}g_{+}Fg_{+}F};g_{+}t_4]^{+}$
-, 0.0, 2.9 kJ/mol

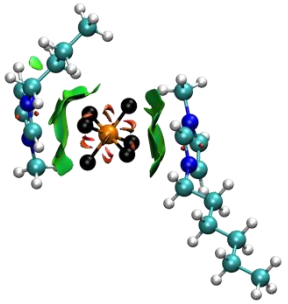

$[g_{+}t_2;\mathbf{g_{+}g_{+}Fg_{+}F};g_{-}t_4]$
-, 3.5, 0.0 kJ/mol

$[C_4mim{:}PF_6{:}C_6mim]^{+}$

Figure S7.

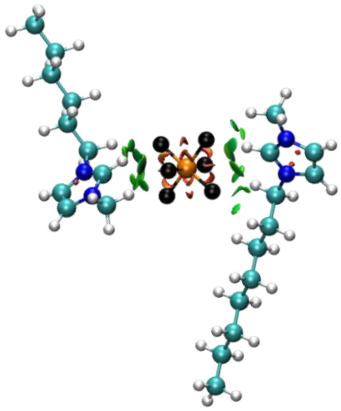

$[g\_t_4;\mathbf{g\_cFcF};g\_t_6]^+$
0.0, -, - kJ/mol

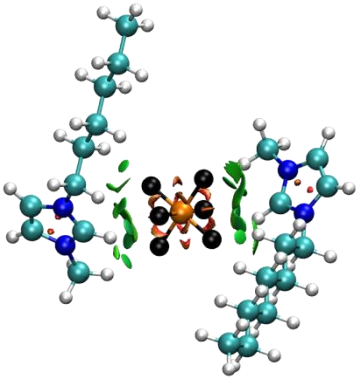

$[g_+t_4;\mathbf{g_+cFcF};g\_t_6]^+$
4.8, -, - kJ/mol

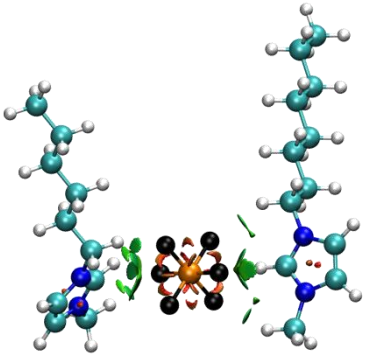

$[g_+t_4;\mathbf{g\_cFcF};g\_t_6]^+$
4.9, -, - kJ/mol

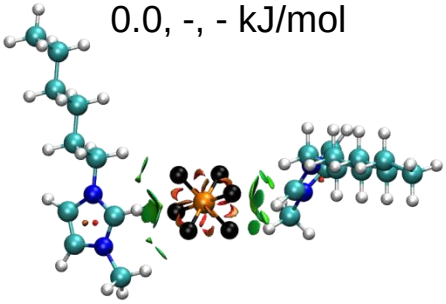

$[g\_t_4;\mathbf{g_+cFcF};g_+t_6]^+$
4.9, -, - kJ/mol

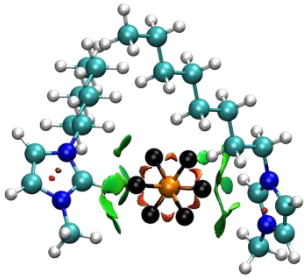

$[g_+t_4;\mathbf{g_+cFcF};g_+t_6]^+$
5.4, -, - kJ/mol

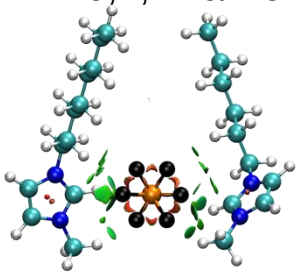

$[g_+t_4;\mathbf{g\_cFcF};g\_t_6]^+$
6.3, -, - kJ/mol

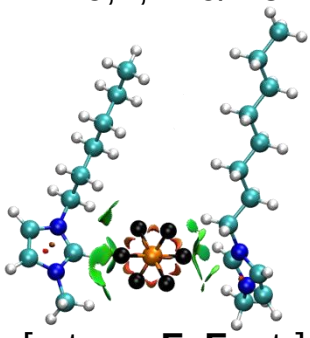

$[g\_t_4;\mathbf{g_+cFcF};g\_t_6]^+$
6.6, -, - kJ/mol

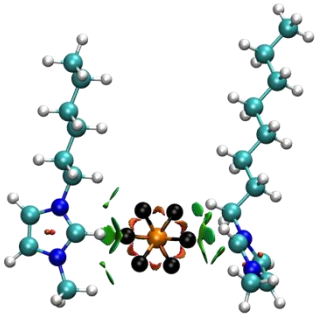

$[g\_t_4;\mathbf{g\_cFcF};g_+t_6]^+$
7.3, -, - kJ/mol

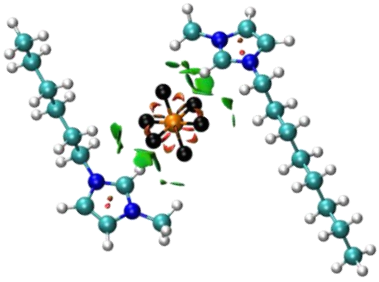

$[g\_t_4;\mathbf{tcFcF};g_+t_6]^+$
7.4, -, - kJ/mol

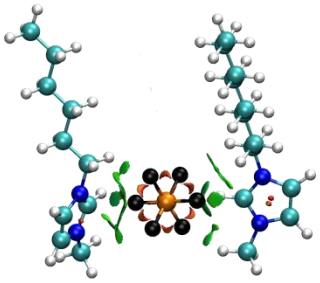

$[g_+t_4;\mathbf{ccFcF};g_+t_6]^+$
7.5 ,-, - kJ/mol

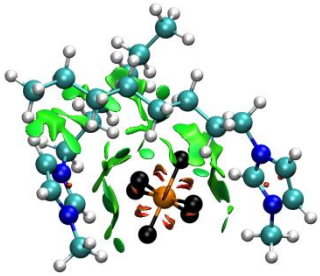

$[g\_t_4;\mathbf{g_+g\_Fg_+F};g_+t_6]^+$
-, 0.0, 10.7 kJ/mol

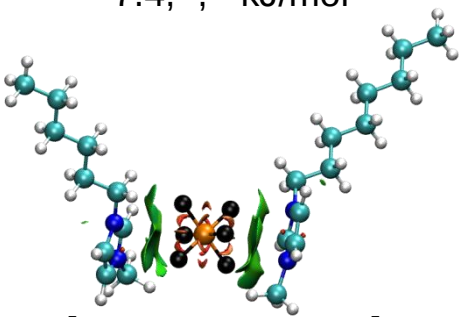

$[g_+t_4;\mathbf{g\_g\_Fg_+F};g\_t_6]^+$
-, 10.5, 0.0 kJ/mol

$[C_6mim{:}PF_6{:}C_8mim]^+$

Figure S8.

B3LYP/6-311+G(d,p)

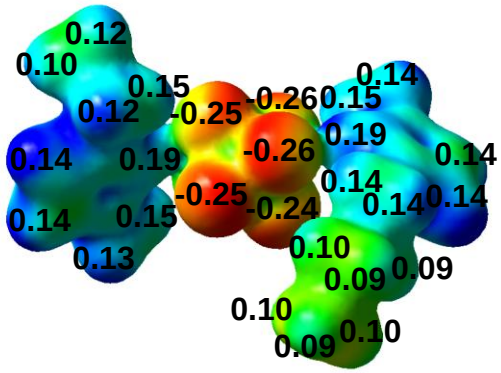

$[g_-;\mathbf{g_-cFcF};g_-t_2]^+$

$[C_2mim:PF_6:C_4mim]^+$

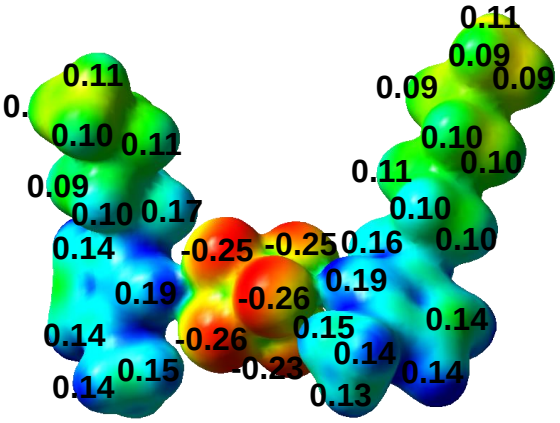

$[g_-t_2;\mathbf{g_-cFcF};g_+t_4]^+$

$[C_4mim:PF_6:C_6mim]^+$

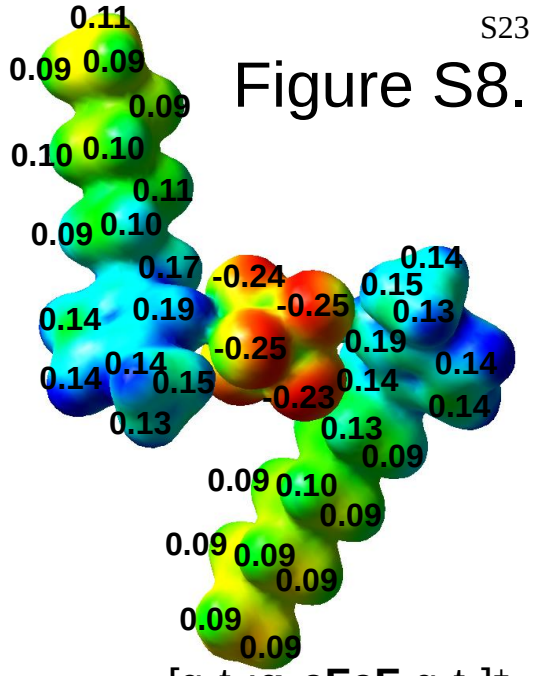

$[g_-t_4;\mathbf{g_+cFcF;}g_-t_6]^+$

$[C_6mim:PF_6:C_8mim]^+$

$[g_-;\mathbf{g_-g_+Fg_-F};g_-t_2]^+$

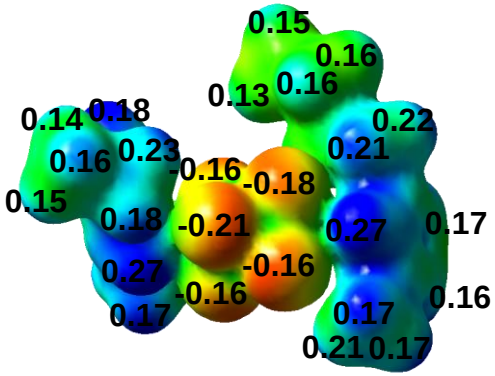

$[g_+t_2;\mathbf{g_+g_+Fg_+F};g_-t_4]^+$

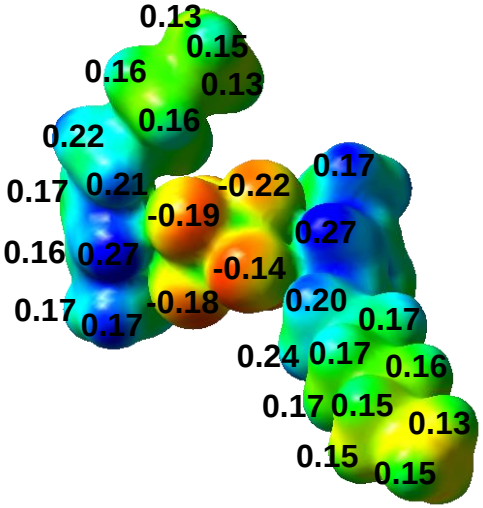

$[g_+t_4;\mathbf{g_-g_-Fg_+F}\ ;g_-t_6]^+$

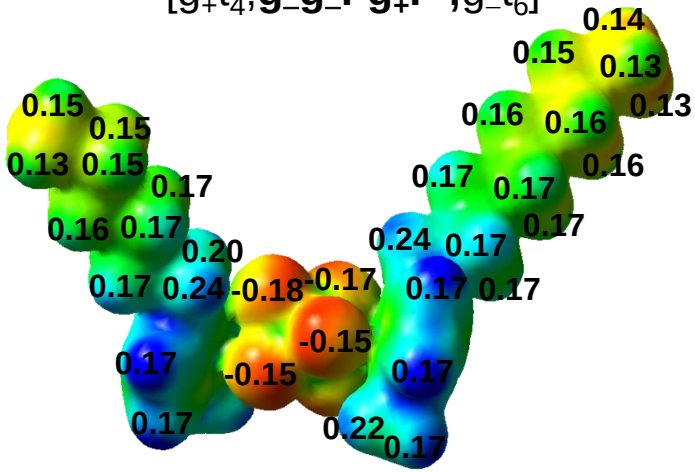

M06-2X/6-311+G(d,p)

Figure S9.

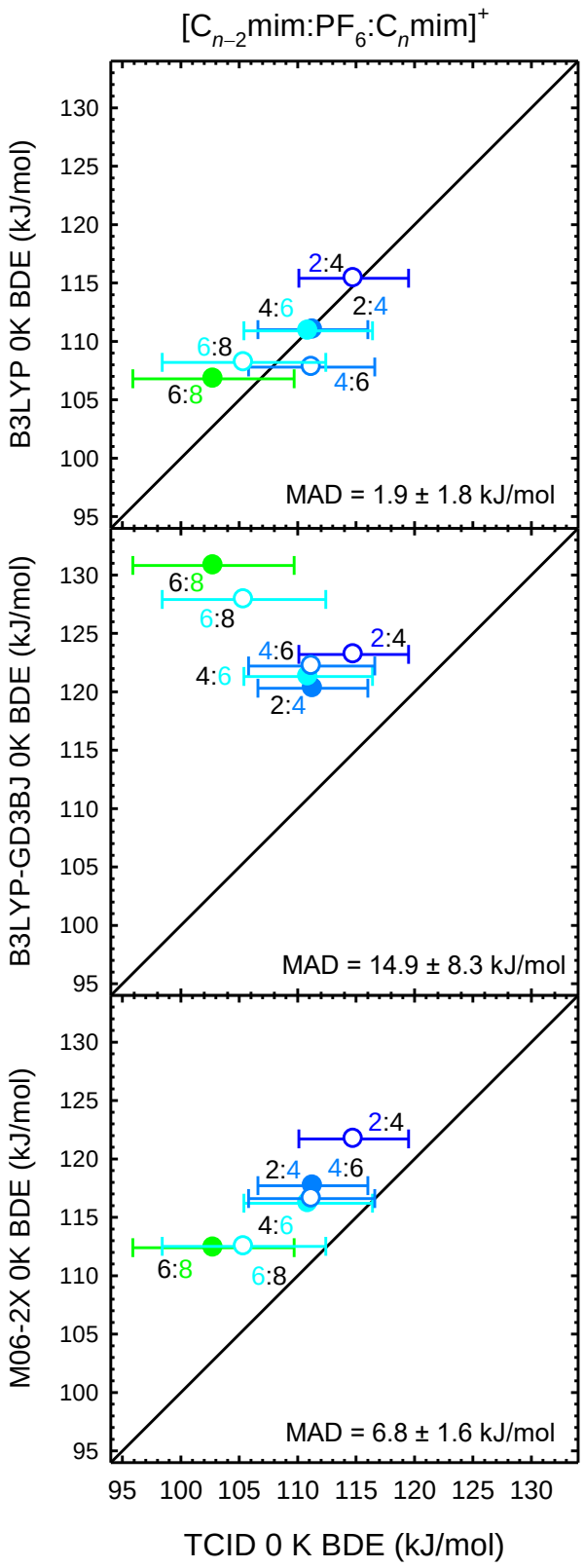
[C$_{n-2}$mim:PF$_6$:C$_n$mim]$^+$
B3LYP 0K BDE (kJ/mol)
B3LYP-GD3BJ 0K BDE (kJ/mol)
M06-2X 0K BDE (kJ/mol)
TCID 0 K BDE (kJ/mol)
MAD = 1.9 ± 1.8 kJ/mol
MAD = 14.9 ± 8.3 kJ/mol
MAD = 6.8 ± 1.6 kJ/mol
2:4
4:6
6:8
95
100
105
110
115
120
125
130

Figure S10.

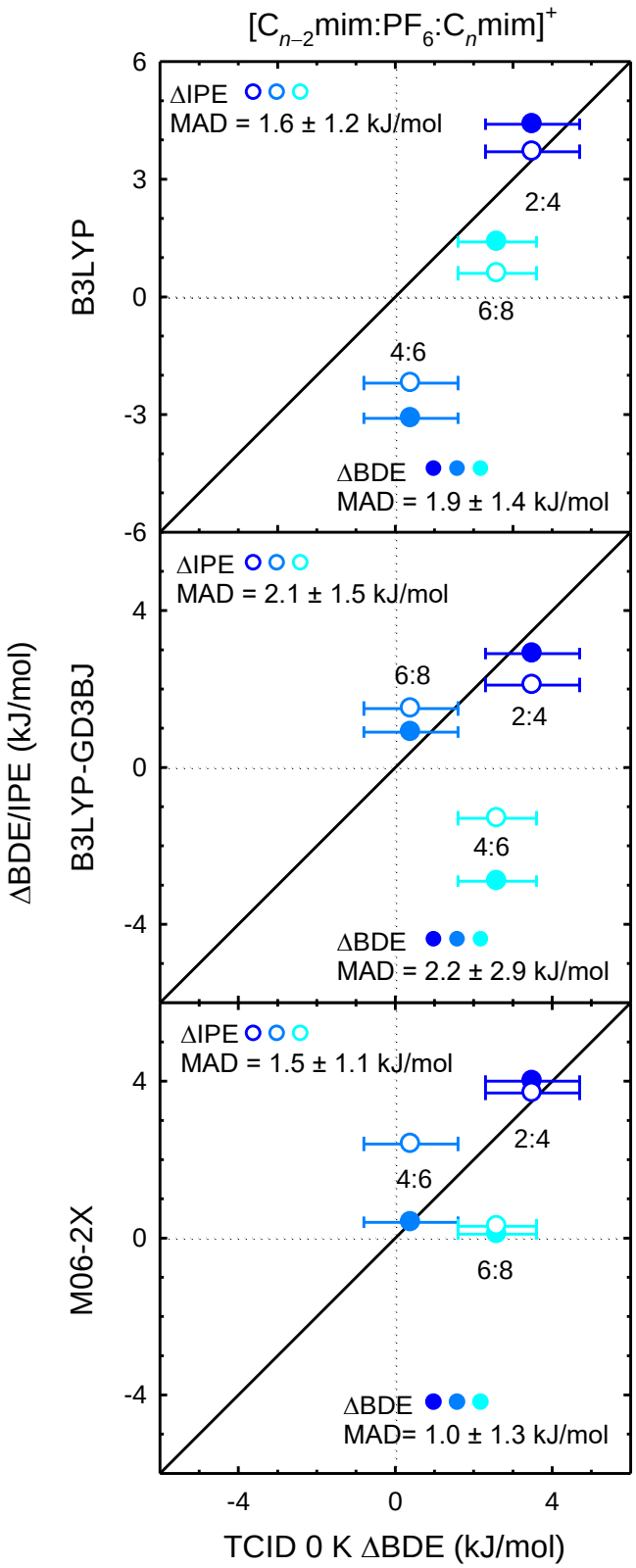
[C$_{n-2}$mim:PF$_6$:C$_n$mim]$^+$
ΔBDE/IPE (kJ/mol)
B3LYP
B3LYP-GD3BJ
M06-2X
ΔIPE
MAD = 1.6 ± 1.2 kJ/mol
2:4
6:8
4:6
ΔBDE
MAD = 1.9 ± 1.4 kJ/mol
ΔIPE
MAD = 2.1 ± 1.5 kJ/mol
6:8
2:4
4:6
ΔBDE
MAD = 2.2 ± 2.9 kJ/mol
ΔIPE
MAD = 1.5 ± 1.1 kJ/mol
2:4
4:6
6:8
ΔBDE
MAD= 1.0 ± 1.3 kJ/mol
TCID 0 K ΔBDE (kJ/mol)

Figure S11.

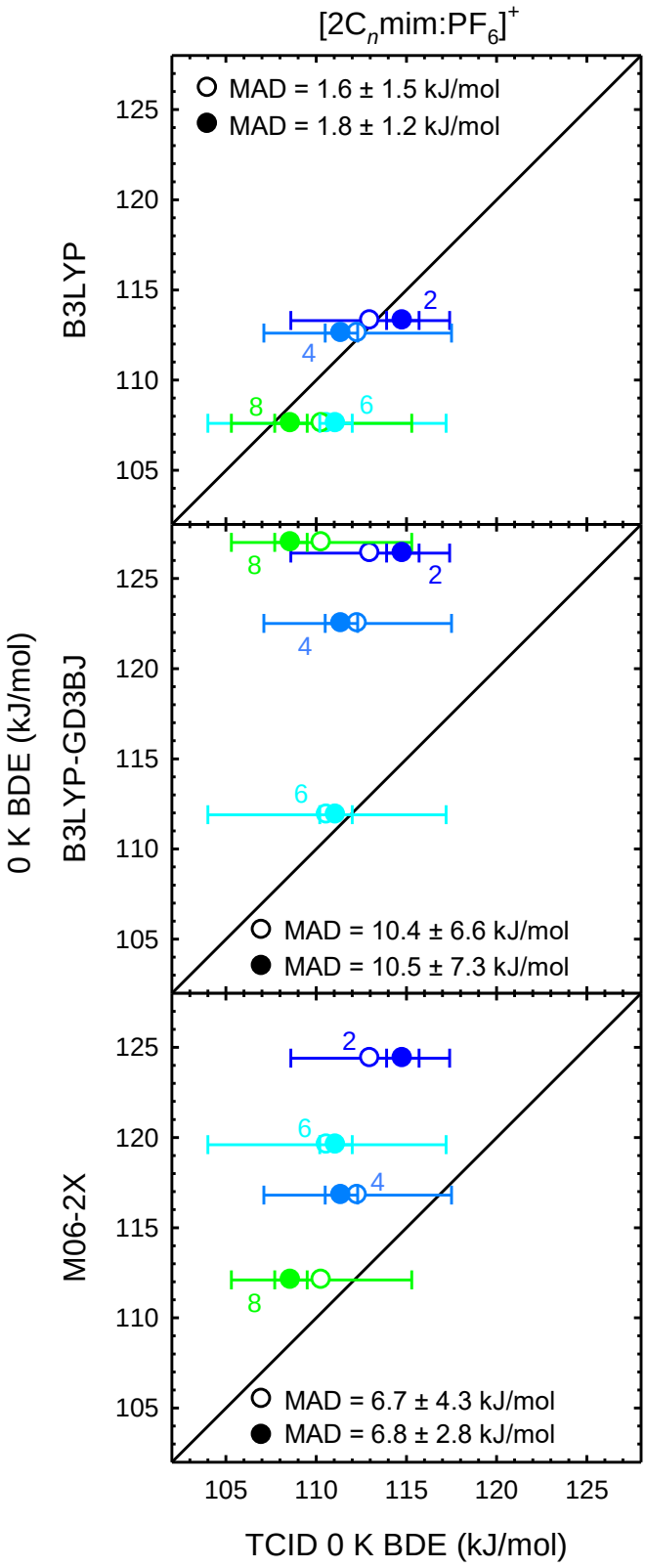
[2C$_n$mim:PF$_6$]$^+$
MAD = 1.6 ± 1.5 kJ/mol
MAD = 1.8 ± 1.2 kJ/mol
B3LYP
MAD = 10.4 ± 6.6 kJ/mol
MAD = 10.5 ± 7.3 kJ/mol
B3LYP-GD3BJ
MAD = 6.7 ± 4.3 kJ/mol
MAD = 6.8 ± 2.8 kJ/mol
M06-2X
0 K BDE (kJ/mol)
TCID 0 K BDE (kJ/mol)
105
110
115
120
125
2
4
6
8